The Plant Journal (2000) **21**(4), 317–327

Maize *high chlorophyll fluorescent 60* mutation is caused by an *Ac* disruption of the gene encoding the chloroplast ribosomal small subunit protein 17

Neil P. Schultes[1,*], Ruairidh J.H. Sawers[2], Thomas P. Brutnell[2,†] and Roger W. Krueger[3,‡]
[1]*Department of Biochemistry and Genetics, The Connecticut Agricultural Experiment Station, 123 Huntington Street, New Haven, CT 06511, USA,*
[2]*Department of Plant Sciences, University of Oxford, South Parks Road, Oxford OX1 3RB, UK, and*
[3]*Department of Molecular, Cellular and Developmental Biology, Yale University, PO Box 208104, New Haven, CT 06511, USA*

Received 6 September 1999; revised 23 December 1999; accepted 5 January 2000.
*For correspondence (fax +1 203 974 8502; e-mail neil.schultes@po.state.ct.us).
[†]Present address: Boyce Thompson Institute for Plant Research, Tower Road, Ithaca, NY 14853, USA.
[‡]Present address: Monsanto, 800 N. Lindberg Blvd, St Louis, MO 63167, USA.

Summary

The maize mutation *high chlorophyll fluorescence 60-mutable 1* (*hcf60-m1*), generated through *Activator* (*Ac*) tagging, has insufficient photosynthetic electron transport. Here we show that the *Hcf60* gene encodes a protein with substantial amino acid similarity to plant plastid and bacterial ribosomal small subunit protein 17 (RPS17) proteins. The lack of detectable *HCF60* transcripts in mutant leaves, and insertion of the transposed *Ac* element 17 bp upstream of the start of translation in the mutated locus, suggest that little if any RPS17 is produced. The mutant phenotype is consistent with reduced plastid translation. Seedling lethal *hcf60-m1* plants display temperature and light-dependent chlorophyll deficiencies, a depletion of plastid rRNA pools, and few high-molecular-weight polysomal complexes. Growth under moderate light conditions (27°C, 100 μE m^{-2} sec^{-1}) allows for substantial chlorophyll accumulation in mutant leaves, yet the number of functional photosystem II complexes appears low. Nevertheless, the presence of a limited but intact C_4 system indicates that some plastid translation occurs.

Introduction

Full chloroplast function is dispensable for short-term viability in higher plants, as endosperm reserves support heterotrophic growth of young seedlings prior to photosynthetic development. Albino plants deficient in plastid ribosomes undergo cell division and expansion as well as organ initiation and development, if supplied with nutrition (Zubko and Day, 1998). The short-term viability of such defective seedlings facilitates identification of genes important for chloroplast development and function through mutagenic screens. Numerous loci involved in plastid development, division, pigment biosynthesis, transcription and RNA processing, photosynthetic function, protein import and light perception have been uncovered (reviewed by Leon *et al.*, 1998; Mullet, 1988; Somerville, 1986). However, there are few higher plant mutations that are known to directly affect plastid translation or plastid ribosomes.

Pigment-deficient mutations in higher plants are often associated with reduced plastid translation or ribosome instability, but most are the result of pleiotropic effects. Disruption of chlorophylls or carotenoids, either through mutation or treatment with bleaching herbicides, results in photo-oxidative damage leading to plastid ribosome depletion and reduced plastid translation (Börner *et al.*, 1976; Mayfield *et al.*, 1986; Reiss *et al.*, 1983). Other mutations have stronger associations to plastid translation, but a direct role is unclear as the primary gene product remains unknown or the function is not evident. Mutations in this category include maize *virescents 3, 12* and *16* which display a cold-sensitive plastid ribosome depletion (Hopkins and Elfman, 1984), and maize *iojap striping 1* (Han *et al.*, 1992; Walbot and Coe, 1979) associated with reduced plastid ribosomes. Close examination of maize *high chlorophyll fluorescence 7, chloroplast*

protein synthesis 1 (*cps1*) and *cps2* mutations reveal significant plastid translation deficiencies, including a depleted plastid ribosome content, a reduced polysome pool and depressed translational efficiency, suggesting that these mutations directly affect plastid translation (Barkan, 1993). The coupling of plastid message RNA processing with translation is revealed in *chloroplast RNA processing 1* (Barkan *et al.*, 1994); however the exact function of the affected locus is unknown.

Only a few mutations in higher plants are known to directly affect plastid ribosomes. The *Arabidopsis thaliana paleface 1* mutant lacks sufficient rRNA methylase activity, resulting in cold sensitivity and plastid ribosome depletion (Tokuhisa *et al.*, 1998). In *Nicotiana,* mutations in the plastid-encoded 16S rRNA and *S12* genes confer antibiotic resistance (Galili *et al.*, 1989; Svab and Maliga, 1991). Here we characterize the first higher plant mutation in a nuclear-encoded plastid ribosomal protein. Through *Activator*-transposable element tagging, the maize *high chlorophyll fluorescent 60-mutable 1* (*hcf60-m1*) mutation was isolated. This unstable pale green seedling lethal mutation exhibits characteristics of plastid ribosomal mutations, including temperature and light-sensitive pigmentation, reduced photosynthetic capacity, reduced plastid ribosome content, and reduced plastid polysome size. Molecular cloning and characterization revealed that the chloroplast ribosomal small subunit protein 17 (RPS17) was disrupted in *hcf60* mutants.

Results

High chlorophyll fluorescence 60 mutant phenotype

Sectored pale green plants were identified in a screen of M_2 families derived from selfed kernels enriched for *Ac* transposition from the *p-vv* locus on chromosome 1S (Dellaporta and Moreno, 1993). Due to the characteristic fluorescence signal, dark-adapted pale green mutant sectors display upon illumination with UV light (325 nm): the mutation was designated *high chlorophyll fluorescence 60* (*hcf60*) (Miles, 1994). The mutation segregates as a recessive trait (52 mutants per 230 total progeny) and is seedling lethal, even though mutant plants often display dark green revertant sectors on otherwise yellow to pale green colored leaves (Figure 1).

Chlorophyll accumulation in *hcf60-m1* mutant seedlings is both temperature- and light-sensitive. Mutants grown at 17°C, 100 $\mu E\,m^{-2}\,sec^{-1}$ appeared albino, those grown under more moderate conditions at 27°C, 100 $\mu E\,m^{-2}\,sec^{-1}$ appeared pale green, and those grown under greenhouse conditions at approximately 24–27°C, <400 $\mu E\,m^{-2}\,sec^{-1}$ appeared very pale green to yellow (Figure 1). Revertant sectors were phenotypically wild-type. Mutant but not revertant tissue was virescent, greening from the leaf tip to the base under moderate conditions, and to a lesser extent under greenhouse conditions. Spectroscopic analysis of chlorophyll content revealed that greenhouse- and low-temperature-grown mutants were severely pigment deficient (Table 1). In contrast, mutant leaves grown under 27°C, 100 $\mu E\,m^{-2}\,sec^{-1}$ contained near-wild-type levels of chlorophyll; older leaves had a higher pigment content but still showed an altered chlorophyll *a*/*b* ratio (Table 1). No gross deficiencies in other photosynthetic pigments relative to chlorophyll *a* content were observed in mutant leaves grown under 27°C, 100 $\mu E\,m^{-2}\,sec^{-1}$, indicating no block in carotenoid synthesis (Table 2). Higher levels of antheraxanthin and zeaxanthin in mutant tissue may reflect a light-stress response and elevated photoprotective pathways (Demmig-Adams and Adams, 1996).

Hcf60 *mutants have reduced photosynthetic capacity*

The high chlorophyll fluorescent phenotype suggested a block in electron transport (Miles, 1994). To further examine this possibility, chlorophyll fluorescent yield measurements were performed on plants grown under moderate conditions in order to probe the functional state of PSII. Dark-adapted wild-type leaf tissue yielded a characteristic low minimal chlorophyll *a* fluorescence (F_o), a sharp rise to maximal fluorescence (F_m) upon illumination with a saturating light pulse, and a gradual relaxation arriving back at the F_o level (Figure 2a). This reflects the change in Q_A, from fully oxidized to reduced state followed by a gradual return to oxidized state. In contrast, dark-adapted mutant *hcf60-m1* leaf tissue displays an aberrant fluorescent transient induction signature marked by an extremely high F_o level, a small F_m peak and a relaxation curve dipping below F_o (Figure 2b). Similar transient signatures were observed for mutants grown under dim illumination (2.5 $\mu E\,m^{-2}\,sec^{-1}$, 27°C), but no appreciable signal was observed for greenhouse-grown tissue (data not shown). Few complete photosystem II (PSII) complexes are functional in *hcf60* mutant leaves, as indicated by low photochemical quenching, q_p (0.51±0.04 mutant versus 0.92±0.01 wild-type); high non-photochemical quenching, q_n (0.7±0.01 mutant versus 0.42±0.06 wild-type); depressed F_v/F_m values (0.16±0.04 mutant versus 0.72±0.02 wild-type); low quantum yield ϕII (0.05±0.01 mutant versus 0.55±0.01 wild-type); and the aberrant mutant fluorescent transient induction signature. Previous reports indicated that *hcf60-m1* also exhibits disruptions in PSI activity (Miles, 1994). Wild-type and *hcf60* mutant leaves grown under moderate conditions were assayed for changes in *in vivo* absorbance at 820 nm in saturating far-red light, an indicator of P_{700} photo-oxidation. Mutant tissue yielded only 40% of the wild-type signal (data not shown). Together these results suggest that both PSI and PSII are severely impaired in the *hcf60* mutant.

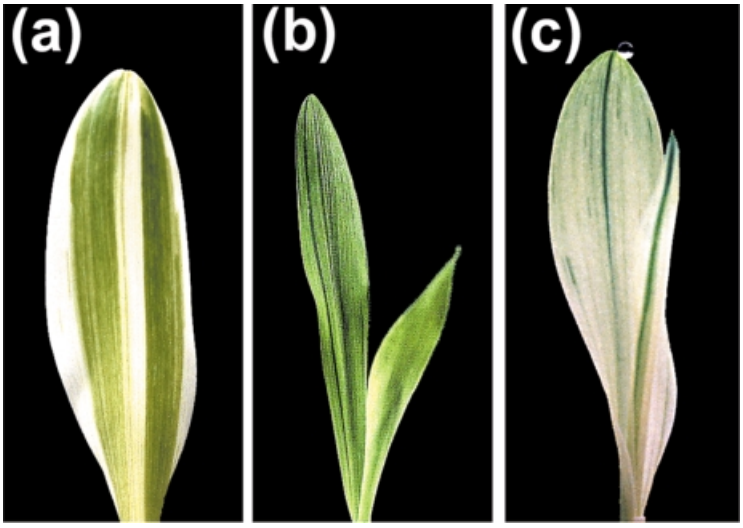

Figure 1. Pigmentation of sectored *hcf60* mutant seedling leaves grown under varying conditions.
(a) Seedlings grown at 17°C, 100 μE m^{-2} sec^{-1}.
(b) Seedlings grown at 27°C, 100 μE m^{-2} sec^{-1}.
(c) Seedlings grown in the greenhouse.

Table 1. Leaf chlorophyll content under different growth conditions

	17°C, 100 μE m^{-2} sec^{-1}		27°C, 100 μE m^{-2} sec^{-1}				Greenhouse	
	1st leaf		1st leaf		2nd leaf		1st leaf	
	WT	*hcf60*	WT	*hcf60*	WT	*hcf60*	WT	*hcf60*
Total chlorophyll μg mg^{-1} tissue	0.385 ± 0.42 *n* = 4	>0.002 ±0.00017 *n* = 4	1.11 ±0.15 *n* = 7	0.79 ± 0.1 *n* = 7	1.3 ±0.2 *n* = 7	0.71 ± 0.17 *n* = 7	0.89 ±0.077 *n* = 4	0.026 ± 0.012 *n* = 3
Total chlorophyll % WT	100	>0.5	100	71	100	55	100	2.9
Chlorophyll *a*/*b*	2.12 ±0.2	–	2.54 ±0.22	1.89 ±0.16	2.65 ±0.26	1.97 ±0.12	3.02 ±0.11	2.87 ±0.23

The low level of photosystem activities suggests that even under mild growth conditions, photosynthesis is severely impaired. To determine if the C_4 photosynthesis cycle is intact and functional, the CO_2 compensation point of *hcf60-m1* leaf tissue was determined. The CO_2 compensation point measures the equilibrium CO_2 concentration achieved between CO_2 fixation into the Calvin cycle and release via respiration of tissue in a closed system. These measurements are dependent on functional light and dark photosynthetic reactions, and are sensitive assays for complete C_4 function. As shown in Figure 3, mutant tissue grown under moderate conditions can achieve a low CO_2 compensation point characteristic of maize and other C_4 plants. However, mutant tissue reaches equilibrium at a slower rate than wild-type tissue, suggesting that the rate of CO_2 fixation is low. Revertant tissue acts as wild-type, whereas greenhouse-grown mutant tissue never achieves equilibrium but continues to accumulate CO_2, indicating that the rate of photosynthesis is insufficient to overcome cellular respiration (data not shown). Mutant tissue samples with no visible revertant sectors were chosen for analysis to minimize the contribution of revertant cells to the analysis.

Table 2. HPLC pigment analysis

	Pigment concentration (mol per 100 mol chlorophyll *a*)			
	1st leaf		2nd leaf	
Pigment	WT	*hcf60*	WT	*hcf60*
Chlorophyll *a*	100	100	100	100
Chlorophyll *b*	33	54	32	51
Lutein	14	15	16	17
Zeaxanthin	nd	2.5	nd	3.5
Antheraxanthin	0.4	2.8	0.4	4.2
Violaxanthin	16	19	30	18

nd, No discernible peak detected on HPLC.
Each data set is from four leaf samples; plants grown at 27°C, 100 μE m^{-2} sec^{-1}.

Hcf60 *is due to insertion of Ac*

The *hcf60-m1* mutation was identified in *Ac*-containing lines in which transpositions were selected and M_2 populations generated. Genetic segregation and DNA blot analysis revealed that a novel transposed-*Ac* element

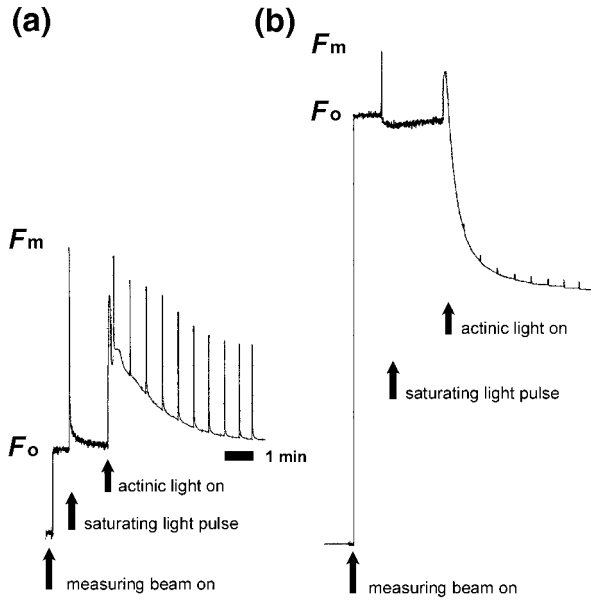

Figure 2. Chlorophyll fluorescent yield measurements.
(a) Chlorophyll fluorescent induction kinetics of dark-adapted wild-type leaf.
(b) Chlorophyll fluorescent induction kinetics of dark-adapted *hcf60-m1* leaf.
F_o and F_m denote the minimal and maximal chlorophyll *a* fluorescence of dark-adapted leaves.

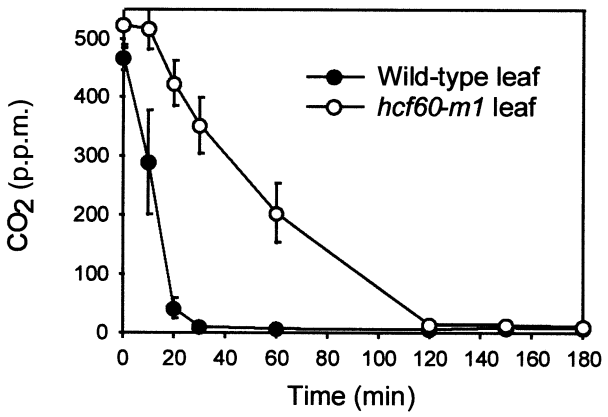

Figure 3. CO_2 compensation point analysis.
Time courses of averaged CO_2 concentration measurements for *hcf60-m1* and wild-type sibling seedling leaf tissue grown at 27°C, 100 μE m^{-2} sec^{-1}. CO_2 concentration is measured in p.p.m.

(tr-*Ac*) cosegregated with the *hcf60* mutant phenotype. In Figure 4(a), DNA from individual plants segregating the *hcf60-m1* phenotype was digested with *Eco*RI, fractionated and probed with *Ac*-specific sequences. The resulting blot shows a novel 4.7 kb band (labeled tr-*Ac*) present in all mutants (lanes 5–10), but segregating among wild-type individuals (lanes 1–4). The tr-*Ac* and adjacent genomic DNA was cloned, and DNA blot analysis reveals that the flanking genomic DNA sequences identify wild-type *Hcf60* and putatively *Ac*-tagged *hcf60-m1* fragments (Figure 4b). In Figure 4(b), DNA from all wild-type individuals displays an 11 kb *Eco*RI DNA fragment (lanes 1–5, black arrow) corresponding to *Hcf60*, and some individuals contain a 4.7 kb *Eco*RI fragment (lanes 3–5, gray arrow) corresponding to *hcf60-m1*. Mutant individuals all display the 4.7 kb *Eco*RI fragment, but lack the wild-type 11 kb *Eoc*RI fragment (lanes 6–10). All individuals contain a cross-hybridizing 4.6 kb *Eco*RI fragment (star). Additional DNA blot analysis of 28 *hcf60-m1* mutants revealed no wild-type 11 kb *Eco*RI fragments (data not shown). These segregation data reveal a close linkage between a novel tr-*Ac* and the *hcf60* mutation.

If the tr-*Ac* were responsible for the mutant phenotype, then excisions of the tr-*Ac* that restored *Hcf60* function would give rise to phenotypically wild-type tissue that would also show the molecular genotype of a heterozygote. In Figure 4(c) DNA from wild-type, mutant and representative revertant sector tissues was digested with *Xba*I, fractionated and probed with flanking genomic DNA. The wild-type sample is a heterozygote containing a *Hcf60* hybridizing band at 12 kb (black arrow) and a *hcf60-m1* band at 6 kb (gray arrow) (lane 1). The mutant sample displays the 6 kp *Ac* fragment (lane 2). Revertant sectors (lanes 3–5) all appear as heterozygotes displaying both the 12 kb *Hcf60 and* 6 kb *hcf60-m1* fragments. We have analyzed DNA isolated from revertant sectors from nine independent mutant plants: all display DNA fragments characteristic of heterozygotes (data not shown). All samples display lower molecular weight cross-hybridizing bands (stars). The results link the restoration of *Hcf60* phenotype with the genotype of *Ac* excision and indicate that the tr-*Ac* is responsible for the mutation.

Comparison of the DNA sequence of *hcf60-m1* genomic DNA with a full-length wild-type cDNA reveals that an *Ac* element has inserted 17 bp upstream from the predicted ATG codon in a region sharing sequence similarity with the *Ac* end (Figure 5a). The *Ac* insertion displaces the *Hcf60* transcription start sites from the coding region. In addition, *Ac* transcription proceeds in the opposite direction from the *Hcf60* coding region, suggesting that read-through transcription is unlikely (Figure 5a). Indeed, RNA blot analysis does not detect *Hcf60* transcript in mutant tissue (Figure 6b).

Hcf60 *encodes the plastid S17 ribosomal protein*

RNA blot analysis reveals that the 0.7 kb *Hcf60* transcript is present in both seedling leaf and root tissue (Figure 6a). A full-length cDNA was isolated and characterized from a maize cDNA library. The 638 bp cDNA clone includes 26 bp of 5′ UTR sequence, a predicted open reading frame of 399 bp followed by 212 bp of 3′ UTR region (Figure 5a). The predicted HCF60 protein shares significant sequence and predicted structural similarity with plant chloroplast and

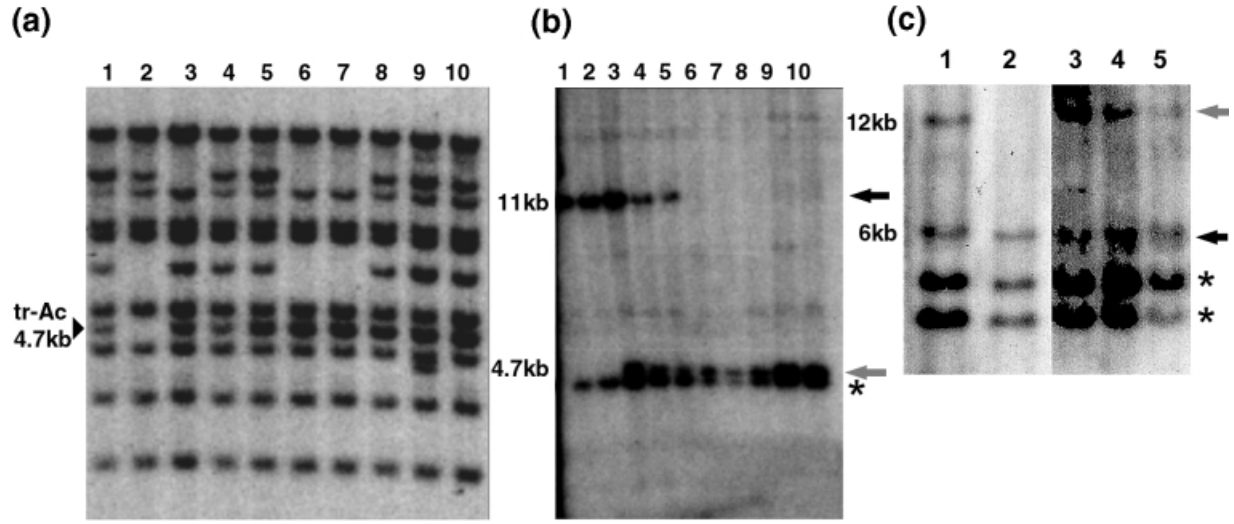

Figure 4. Association of an *Ac* insertion with the *HCF60* locus.
(a) Segregation analysis with an *Ac* probe. A novel 4.7 kb DNA restriction fragment containing a transposed *Ac* (tr-*Ac*) was detected in a family segregating *hcf60* mutant phenotypes. Lanes 1–4 contain genomic DNA from wild-type seedlings digested with *Eco*RI. Lanes 5–10 contain genomic DNA from *hcf60* mutant seedlings digested with *Eco*RI. The DNA blot was probed with internal 700 bp *Eco*RI–*Hin*dIII *Ac* sequences.
(b) Segregation analysis with flanking genomic DNA. Genomic DNA flanking the novel tr-*Ac* was used as a probe (pNS274). Lanes 1–5 contain genomic DNA from wild-type seedlings digested with *Eco*RI. Lanes 6–10 contain genomic DNA from *hcf60* mutant seedlings digested with *Eco*RI. Black arrows denote *Hcf60* DNA fragments; gray arrows *hcf60-m1* DNA fragments.
(c) Revertant sector analysis. Lanes 1 and 2 contain genomic DNA from heterozygous wild-type and *hcf60* mutant seedling, respectively, digested with *Xba*I. Lanes 3–5 contain genomic DNA from somatic revertant sectors isolated from different *hcf60* mutant tissue, digested with *Xba*I. DNA blot was probed as in (b). Black arrows denote *Hcf60* DNA fragments; gray arrows *hcf60-m1* DNA fragments.

many prokaryotic 30S ribosome subunit S17 proteins (Figure 5b) (Altschul *et al.*, 1997). Analysis of the mutant genomic locus reveals no intron sequences in the predicted coding region (data not shown), as also observed for the homologous *Arabidopsis Rps17* locus (Thompson *et al.*, 1992). Pairwise alignments show high levels of identity with rice RPS17 (63/71% identity/similarity), *Arabidopsis* RPS17 (54/71%) and pea RPS17 (44/75%), and lower ranges with representative prokaryotic *Bacillus stearothermophilus* (26/43%), *Escherichia coli* (28/47%) and *Thermus thermophilus* (38/44%) S17 proteins. Overall secondary structures in the core of the proteins are conserved. Predicted β-sheet regions overlap among the S17 proteins and align with the five β-sheet domains observed in the tertiary structure of *B. stearothermophilus* S17 (data not shown) (Golden *et al.*, 1993). Hydrophobic amino acids in the core of the protein are conserved (Figure 5b, circles) (Golden *et al.*, 1993), and positively charged amino acids believed to interact with rRNA are also conserved (Figure 5b, plus) (Jaishree *et al.*, 1996). Key residues identified by mutational analysis are also conserved among all S17 proteins, including the histidine involved in neamine resistance (Figure 5b, solid arrow) (Yaguchi *et al.*, 1976) and serine important in temperature sensitivity (Figure 5b, open arrow) (Herzog *et al.*, 1979).

It is likely that the extra N-terminal residues common to all plant RPS17 proteins and lacking in prokaryotic S17 proteins correspond to chloroplast transit sequences. The HCF60 N-terminus exhibits amino acid composition and distribution characteristic of transit sequences (Cline and Henry, 1996) and is predicted to contain a chloroplast transit peptide cleaved at amino acid 43 (Emanuelsson *et al.*, 1999). In addition, cleavage and import of pea RPS17 protein occurs in the presence of isolated chloroplasts (Gantt and Key, 1986), supporting the plastid localization of plant RPS17 proteins.

Chloroplast ribosomes are depleted and polysome size is reduced in hcf60-m1

If HCF60 were a component of the chloroplast ribosome complex, its absence in *hcf60* mutant plants would probably reduce the translational potential of *hcf60* chloroplasts. Steady-state levels of *Hcf60* transcript were monitored through RNA blot analysis to determine gene expression profiles in wild-type and mutant tissue. In wild-type seedlings the gene is expressed in roots and etiolated leaves and strongly in green leaves (Figure 6a), as has been observed for the *Arabidopsis Rps17* gene (Thompson *et al.*, 1992). However, no transcript is detected in mutant leaf tissue grown under greenhouse conditions or even under moderate conditions (Figure 6b, lanes 2, 4 and 6) despite being abundant in similarly grown wild-type leaves (Figure 6b, 1, 3 and 5). Northern analysis also revealed that in *hcf60* mutant leaves, transcript for *rbcL* is depleted compared to the wild-type, whereas message

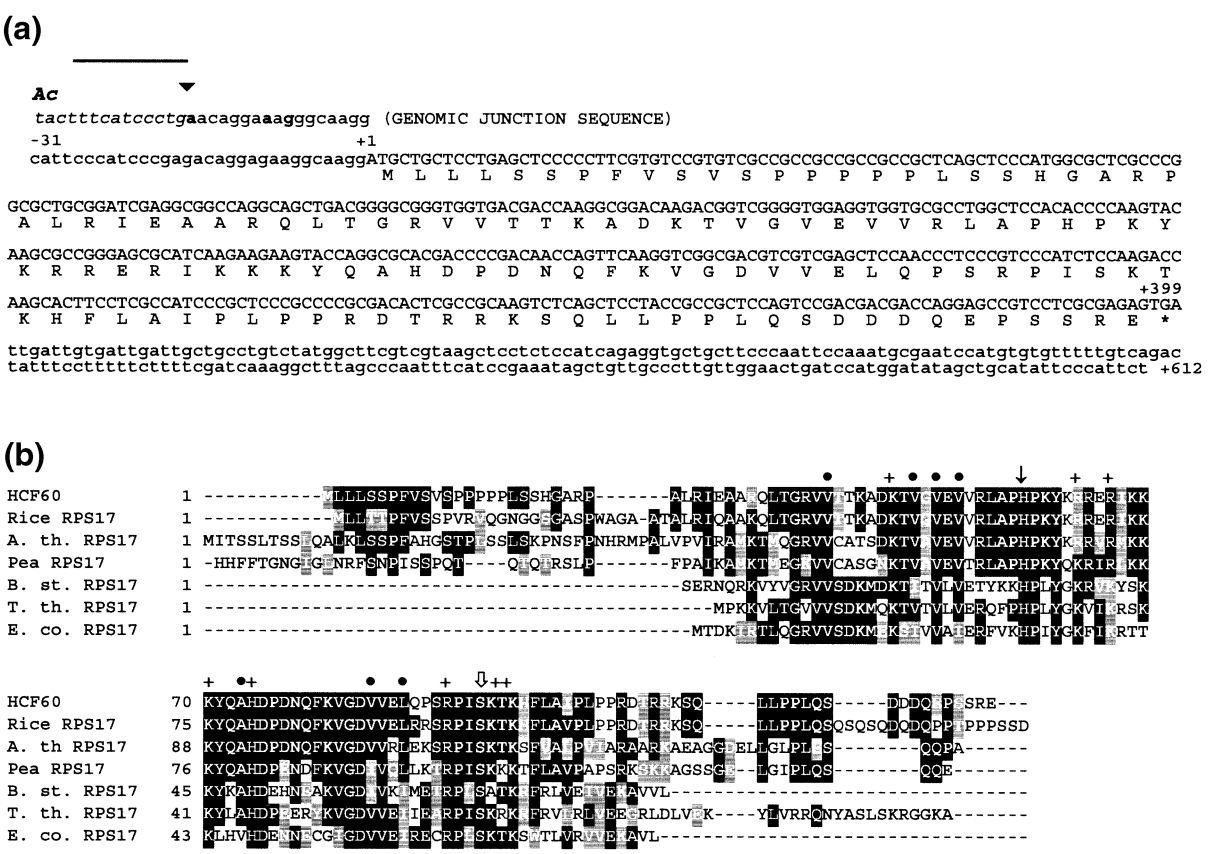

Figure 5. HCF60 sequence analysis.

(a) DNA sequence of *HCF60* locus. Capital letters indicate coding region and deduced amino acid sequence for HCF60; lower case letters represent 5′ and 3′ untranslated regions of the *HCF60* cDNA. Genomic junction sequence aligns the *Ac*-tagged *hcf60-m1* sequence above the wild-type cDNA sequence in the 5′ region. Italic characters and arrow indicate *Ac* sequences; triangle, insertion site; bold characters, bp differences between the genomic and cDNA 5′ UTR sequences. The EMBL accession number is Y19204.

(b) Amino acid sequence alignment of RPS17 proteins. CLUSTALW alignment of maize HCF60 with plant RPS17 and representative bacterial RPS17 proteins (Thompson *et al.*, 1994). Black boxes denote amino acid identity; shaded boxes, amino acid similarity. Solid arrow indicates conserved amino acid involved in neamine resistance; open arrow, conserved amino acid important for temperature sensitivity. Circles denote conserved hydrophobic residues; plus marks conserved charged amino acids. Rice RPS17 (gb# 3777598); A. th. (*Arabidopsis thaliana*) RPS17 (sp.# P16180) (Gantt and Thompson, 1990); pea RPS17 (sp.# P17092) (Gantt and Thompson, 1990); B. st. (*Bacillus stearothermophilus*) RPS17 (gb# 443236) (Herfurth *et al.*, 1991); E. co. (*Escherichia coli*) RPS17 (sp.# P02373) (Yaguchi and Wittmann, 1978); T. th. (*Thermus thermophilus*) RPS17 (sp.# P24321) (Jahn *et al.*, 1991). Alignment presentation with BOXSHADE 3.2.

accumulation for *atpB* is unaffected (Figure 6c). Destabilization of *rbcL* message has been observed in mutants affecting chloroplast ribosome content and polysome accumulation (Barkan, 1993).

Previous studies have also correlated reduced plastid rRNA accumulation with a reduced polysomal content (Barkan, 1993). rRNA levels were compared between *hcf60* mutant and wild-type plants. Ribosomal RNAs were monitored by electrophoresis to determine the relative abundance of cytoplasmic versus plastid ribosomes. As expected, wild-type leaf tissue contains abundant plastid rRNA due to high numbers and size of functional chloroplasts as compared to wild-type root rRNA (compare 1.6 and 1.15 kb RNA, Figure 7a, lanes 1 and 2). In contrast, mutant leaf tissue is severely depleted in chloroplast rRNA when grown under greenhouse or even moderate conditions (Figure 7a, lanes 3 and 4). Digitized image analysis shows that mutant leaves contain less plastid rRNA than is present in wild-type leaves (comparing the ratios of the 3.2 kb cytoplasmic rRNA and plastid 1.6 kb RNA fragments). Mutant leaves grown under moderate conditions contain 14% (±1.5, $n=3$) and mutant leaves grown under greenhouse conditions contained 12.8% (±5.3, $n=5$) wild-type levels of rRNA.

To examine the role of HCF60 in plastid polysome accumulation, leaf extracts were isolated from wild-type and mutant *hcf60* tissue and fractionated over sucrose gradients prior to RNA blot analysis (see Experimental procedures). In wild-type leaves, *rbcL* and *atpB* transcripts are predominantly associated with large polysomes, while in *hcf60* mutant leaves the bulk of these transcripts are associated with monosomes or are present as free RNA species (Figure 7b). The decreased number of plastid ribosomes is probably due to inefficient translation initia-

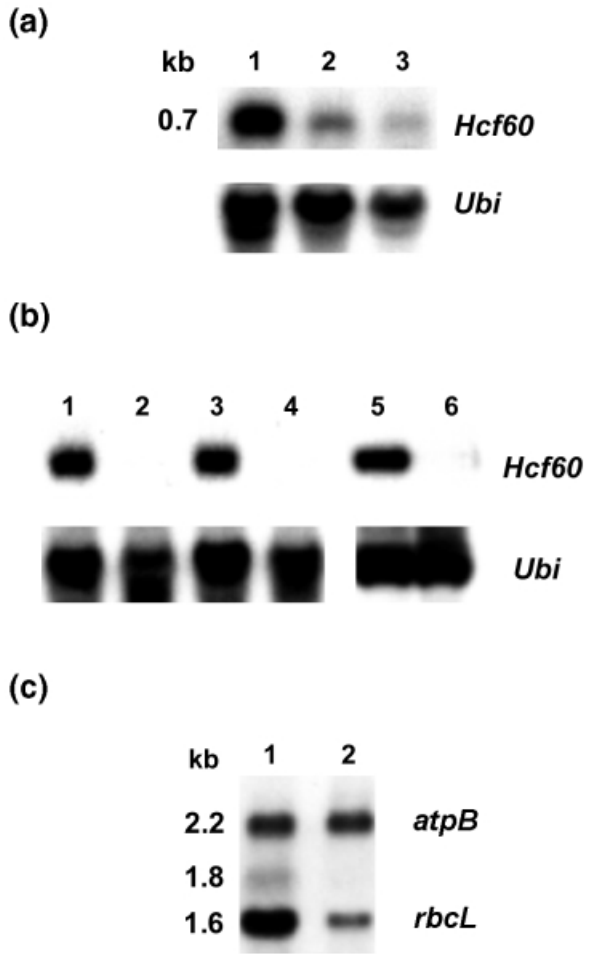

Figure 6. Gene expression analysis.
(a) Tissue expression of *HCF60*. Lane 1 contains RNA from wild-type green seedling leaf; lane 2, RNA from wild-type etiolated seedling leaf; lane 3, RNA from wild-type seedling root, probed with *Hcf60* cDNA (pHCF60–7B) or ubiquitin (*ubi*) sequences. All lanes contain approximately 5 μg total RNA.
(b) Expression of *HCF60* in mutant tissue. Lanes 1, 3 and 5 contain RNA from wild-type maize seedling leaves. Lanes 2, 4 and 6 contain RNA from sibling *hcf60* mutant seedling leaves. Seedlings were grown under greenhouse conditions (lanes 1–4) or at 27°C 100 μE m^{-2} sec^{-1} (lanes 5 and 6). RNA blots probed with *HCF60* and *ubi* sequences. All lanes contain approximately 5 μg total RNA.
(c) Plastid transcription. Expression of plastid-encoded *atpB* and *rbcL* genes was monitored in wild-type (lane 1) and *hcf60* mutant (lane 2) sibling seedling leaves. RNA blot was probed with *atpB* (2.2 kb) and *rbcL* sequences (1.6 and 1.8 kb).

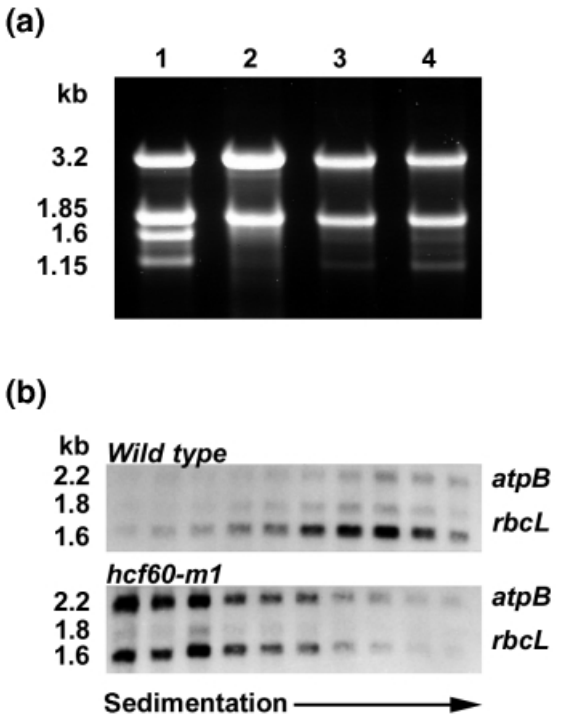

Figure 7. Chloroplast ribosome and polysome analysis.
(a) rRNA comparison. Total RNA was isolated from wild-type greenhouse-grown seedling leaf (lane 1), root (lane 2), and *hcf60* mutant leaf grown in the greenhouse (lane 3) or at 27°C, 100 μE m^{-2} sec^{-1} (lane 4). Cytoplasmic rRNA forms correspond to 3.2 and 1.85 kb; organelle rRNA corresponds to 1.6 and 1.15 kb RNAs. 2 μg total RNA were denatured and run on a native 1 × MOPS agarose gel.
(b) Polysome accumulation. RNA blots containing fractionated aliquots of sedimented wild-type or *hcf60-m1* leaf tissue were probed with *rbcL* and *atpB* sequences. Arrow indicates increasing sedimentation of fractions.

tion rather than inefficient translation elongation. Altered translation elongation would tend to accumulate large polysomes, as has been observed in cells treated with ribosome translation inhibitors and in maize *bundle sheath defective 2* mutant tissue (Brutnell *et al.*, 1999; Klaff and Gruissem, 1991).

Hcf60 *locates to chromosome 8L*

The *Hcf60* locus was mapped to chromosome 8L in crosses employing B–A translocation lines (Beckett, 1978). Mating between *hcf60* heterozygotes and lines carrying TB-8La or TB-8Lc translocations resulted in pale green, often somatically unstable F_1 progeny at 6% (19/219) and 8.3% (128/1543), respectively. Crosses between *hcf60-m1* heterozygotes and maize lines harboring other mutations mapping to chromosome 8L and exhibiting high chlorophyll fluorescent, virescent or pigment-deficient phenotypes (including *hcf102*, *virescent 16* and *21*, *japonica 1*, *yellow-024-5*, *white lutens 3*, *white 0-53-4*, *w0-34-16* and *w8963*) resulted in complementation in the F_1 progeny, establishing that *hcf60-m1* is not allelic.

Discussion

Both the plastid and nuclear genomes encode plastid ribosomal proteins (RPs). Of the approximately 60 plastid RPs in higher plants, 21 are plastid encoded, and 16 of the remaining 39 nuclear-encoded RPs have been characterized (reviewed by Subramanian, 1993; Sugiura *et al.*, 1998). We have shown that the maize *hcf60-m1* mutation is caused by *Ac* insertion into the *Rps17* locus, and is one of

the few higher plant mutations directly affecting plastid ribosome proteins.

Genetic, molecular and gene expression data all support the conclusion that an *Ac* insertion is responsible for the *hcf60* mutant phenotype. An *Ac* insertion was identified that showed linkage with the mutant phenotype, and somatic excisions of this element restored a wild-type phenotype. The insertion of *Ac* in the *hcf60* 5′ UTR region displaces promoter and the putative transcription start site approximately 4.5 kb from the coding region of the gene. Furthermore, no *Hcf60* transcript was observed in mutant tissue, which retains photosynthetic capacity. Nuclear and plastid translation must still occur in such mutant tissue. Together these data suggest that an *Ac*-induced disruption of *Hcf60* transcription results in the mutant phenotype and gene expression profile.

Hcf60 encodes a plastid RPS17 protein, as clearly deduced from the high level of amino acid sequence similarity, common secondary structures and conserved key amino acids important for structure and function shared with other plant and bacterial RPS17 proteins. Nuclear magnetic resonance structure data for bacterial S17 protein (Golden *et al.*, 1993; Jaishree *et al.*, 1996), and cross-linking studies with bacterial ribosomes (Urlaub *et al.*, 1997), place the S17 protein in the 30S subunit interacting with the 16S rRNA molecule. RPS17 is believed to be involved in ribosome assembly (Herzog *et al.*, 1979) and translational fidelity (Yaguchi *et al.*, 1976).

Light- and temperature-dependent leaf pigment content, altered chlorophyll *a*/*b* ratios, virescence and high chlorophyll fluorescence are common among higher plant mutants which directly or indirectly affect plastid ribosome integrity and translational activity. Depressed photochemistry and a lower overall rate of photosynthesis suggest that the *hcf60* lesion does not affect a specific photosynthetic component, but is consistent with reduced levels of many photosynthetic components. The high chlorophyll fluorescent phenotype indicates that electron flow through or subsequent to PSII is inadequate for the level of excitation. Aberrant chlorophyll fluorescence induction signals also indicate that photochemically competent PSII complexes are rare. Relaxation of fluorescence below the F_o level, a high level of non-photochemical quenching and a low PSII quantum yield suggest a dissociation of peripheral PSII antenna complexes from light-harvesting units or excited PSII complexes that are unable to siphon off excess electrons through electron transport. *Arabidopsis hcf109, 110 and 114* mutants all exhibit similarly aberrant chlorophyll fluorescent induction profiles, and are all depleted in PSII components (Meurer *et al.*, 1996). Mutant leaf tissue appears to have reduced PSI activity, as observed from reduced absorption and relaxation signals of mutant tissue exposed to pulses of far-red light, and from previous reports (Miles, 1994). Despite the severely depressed photochemistry, a low CO_2 compensation equilibrium point can be achieved in non-light-stressed mutant tissue. This indicates that intact photochemistry, a complete Calvin cycle and C_4 photosynthetic machinery is present and functioning. The extremely slow rate of attaining CO_2 equilibrium indicates that these photosynthetic enzymes and complexes are limited.

The low steady-state levels of polysome-associated *rbcL* and *atpB* transcripts in *hcf60* mutants suggest that HCF60 is required for polysome accumulation. Plastid ribosomal RNA content in mutant leaf tissue is at least eightfold lower than in wild-type leaf tissue, and reflects either increased turnover of unassembled rRNA or lower levels of rRNA transcription due to reduced plastid translation in mutant tissue. As with other maize mutants that affect plastid ribosomes, *rbcL* transcripts accumulate at low levels (Barkan, 1993; Brutnell *et al.*, 1999). The depletion of rRNA and polysome pools indicates that plastid translation is compromised. A deficit in photosynthetic membrane complexes and enzymes results in poor photosynthetic capacity and other phenotypes discussed above. Nevertheless, low levels of photosynthetic activity are still present.

The data support the hypothesis that *hcf60* plastid ribosome reduction and polysome accumulation result from a deficit or lack of RPS17; however the absence or depletion of this protein from ribosomes has yet to be confirmed. Plastid translation may be compromised, either because insufficient RPS17 is present and few ribosomes accumulate, or because ribosomes that lack RPS17 function poorly. It is possible that a duplicate maize *Rps17* gene is expressed and yields low levels of RPS17. Maize DNA blots probed with *Hcf60* and flanking genomic sequences reveal the presence of several DNA bands (data not shown and Figure 4b,c), suggesting additional *Rps17*-like genes. However, similarly probed RNA blots clearly show that little if any transcript is produced in mutant tissue, indicating that any closely related *Rps17*-like genes are not expressed at a high level. Any additional *Rps17*-like genes producing RPS17 would exhibit reduced nucleic acid sequence similarity to *Hcf60*.

Alternatively, plastid ribosomes which lack RPS17 may function poorly. Plastid and bacterial ribosome function is resilient, and can withstand loss or mutation of a number of protein components and still function. The *tsp-1* mutation in *Chlamydomonas reinhardtii* confers resistance to thiostrepton and results in the loss of plastid ribosomal protein L23 (homologue of bacterial ribosomal protein L11) and slow growth (McElwain *et al.*, 1993). In *E. coli*, mutants that lack any of 16 ribosomal proteins are nevertheless viable and slow-growing (Dabbs, 1991). Through a variety of immunological tests, one such *E. coli* mutant was found to lack ribosomal proteins S17 and L29 (Dabbs *et al.*, 1983; Stöffler-Meilicke *et al.*, 1985). This

is consistent for a role of ribosomal proteins guiding rRNA molecules into proper three-dimensional structures critical for ribosome function (Stern *et al.*, 1988). The loss of any particular protein (such as HCF60) would compromise the efficiency of translation but not prevent it altogether.

It is interesting to note that of the 16 dispensable ribosomal genes in *E. coli*, 15 of the plant homologues are encoded in the nucleus (Subramanian *et al.*, 1990). This correlation supports the hypothesis (Barkan, 1993) that additional higher plant mutations which affect ribosome stability or polysome accumulation, or diminish plastid translation, disrupt other nuclear-encoded plastid ribosome protein genes.

Experimental procedures

Maize stocks and genetics

The *Activator* (*Ac*) transposon mutagenesis strategy used to generate *hcf60-m1 has* been described previously (Dellaporta and Moreno, 1993). Mutant *hcf60*-m1 plants were back-crossed to W22 maize lines and thereafter selfed. Maize stocks obtained from the Maize Cooperation Stock Center (Urbana, IL, USA) include *yellow-024-5* (#801I); *v16* and *v21* (#801B and 804A); *japonica 1* (#810B); *white lutens 3* (#827J); *white 0-53-4* (#804D); *w0-34-16* (#804F); *w8963* (804H); TB8-La (#806A); TB-8Lc (#809A); and *hcf120* (Donald Miles, University of Missouri, USA).

Maize was grown at The Connecticut Agricultural Experiment Station, Hamden, CT, USA during the summers of 1990–98. Seedlings were grown under greenhouse conditions or in growth facilities at the indicated temperature and light conditions under 16 h light/8 h dark conditions in MetroMix 200 (Scotts-Sierra Horticultural Products Company, Maryville, OH, USA).

Pollen from plants carrying B–A translocations affecting chromosome 8L arms was scored as semiviable and used to fertilize heterozygous *hcf60* plants. For complementation crosses, plants homozygous or heterozygous for chromosome 8L mutations were selfed and used as recipients for pollen from selfed wild-type individuals in an *hcf60* segregating family. Progeny were grown in sand benches under greenhouse conditions, and scored.

Pigment analysis

Four 8 mm diameter leaf discs from the first or second leaf of 10-day-old seedlings grown under greenhouse conditions, at 27°C, 100 μE m^{-2} sec^{-1}, or from 24-day-old seedlings grown at 17°C, 100 μE m^{-2} sec^{-1}, were extracted in 80% acetone at –20°C for total chlorophyll determination. Total chlorophyll concentration was determined using a Spectronic Genesys 5 spectrometer (Spectronics Instruments Inc, Rochester, NY, USA) and calculated according to Arnon (1949). For pigment analysis, similar amounts of leaf tissue from seedlings grown at 27°C, 100 μE m^{-2} sec^{-1} were extracted in 85% acetone at –20°C. Individual pigments were separated by reverse-phase HPLC analysis as described by Peterson and Havir (2000).

Light measurements

Chlorophyll fluorescence yield and changes in far-red light absorbance were measured using the Walz pulse amplitude modulation system (H. Walz, Heffeltrich, Germany) as previously described (Peterson, 1994; Peterson and Havir, 2000). For chlorophyll fluorescence yield measurements, 10-day-old seedlings grown at 27°C, 100 μE m^{-2} sec^{-1} were dark-adapted for several hours prior to measurement. Leaves were assayed in a Walz probe given a saturating pulse at 6500 μmol photons m^{-2} sec^{-1} for 0.7 sec, then were superimposed with actinic illumination at 110 μmol photons m^{-2} sec^{-1} at 30 sec intervals. Modulation frequency of the measuring beam was 1.6 kHz for F_o measurements, and was set at 100 kHz for all other measurements. For ΔA_{830} far-red determinations, *hcf60* mutant and wild-type leaves were measured as previously described (Peterson, 1994).

CO_2 compensation point data

Four 5 mm diameter leaf discs from 2-week-old seedlings grown under greenhouse conditions or at 27°C, 100 μE m^{-2} sec^{-1} were placed on wet Whatmann no. 3 MM paper in 50 ml syringes at 27°C, 100 μE m^{-2} sec^{-1}. At timed intervals, 5 ml samples were withdrawn and analyzed in an infrared analyzer (Model 865; Beckman, Palo Alto, CA, USA) over a period of 3 h to ensure that the CO_2 concentration had reached equilibrium, as previously described (Schultes *et al.*, 1996). Data were derived from two or three independent samples.

Nucleic acid manipulation

Maize genomic DNA was prepared as described by Chen and Dellaporta (1993). Total RNA was isolated with TRIzol (Gibco BRL, Gaithersburg, MD, USA) according to the manufacturer's recommendations. DNA was fractionated on agarose gels (Ausubel *et al.*, 1989) and transferred to Zetaprobe GT membrane (Bio-Rad, Richmond, CA, USA) according to the manufacturer. Total RNA was fractionated on formaldehyde agarose gels prior to transfer to Zetaprobe GT membrane and RNA blot analysis. Probes for DNA and RNA hybridization analysis were labeled with ^{32}P-dCTP by random priming (Feinberg and Vogelstein, 1984). Hybridization conditions for DNA and RNA blots were as previously described (Brutnell and Dellaporta, 1994). The genomic 4.7 kb *Eco*RI *Ac*-tagged *hcf60* locus was cloned into pBSK (Stratagene, La Jolla, CA, USA) generating plasmid DPG1846. From DPG1846 a 0.7 kb *Bam*HI–*Cla*I fragment flanking the *Hcf60-m1* coding region and a 1.5 kb *Bam*HI–*Cla*I fragment containing *hcf60-m1* and *Ac* sequences were subcloned into pBSK to generate pNS274 and pNS275, respectively. PNS275 insert was used to screen approximately 400 000 plaques from a B73 maize cDNA library derived from vegetative apices (courtesy of J. Langdale University of Oxford, UK) to isolate wild-type *HCF60* cDNAs. Approximately 20 clones were isolated and the DNA sequence of a full-length 0.7 kb clone (pHCF60–7B) was obtained (W.M. Keck, Biotechnology Resource Laboratory, Yale University, USA). DNA and protein sequence information were analyzed on Lasargene software (DNASTAR Inc., Madison, WI, USA). PSKUBI, containing maize ubiquitin DNA sequences, was used as a control in RNA blots (Christensen *et al.*, 1992). Comparison of plastid rRNA was determined by fractionating serial dilutions of denatured total RNA on agarose gels for each sample. Digitized image of the ethidium bromide-stained gels was captured on The Imager (Appligene, Pleasanton, CA, USA). The ratio of the 1.6 kb organelle rRNA relative to the 3.2 kb cytoplasmic rRNA was determined for each sample using public domain NIH Image v1.61 software. Average values reflect analysis of at least three independent samples.

Polysome experiments

Polysomes were isolated from leaf tissue as previously described (Brutnell *et al.*, 1999). RNA was fractionated on 1.2% agarose formaldehyde gels, blotted onto Nylon membranes and hybridized with a ^{32}P-labeled DNA fragment of maize chloroplast DNA (pZMC460) that recognizes *rbcL* and *atpB* sequences.

Acknowledgements

We would like to thank Richard Peterson (Connecticut Agricultural Experiment Station, New Haven, CT) for assistance with transient fluorescent measurements, Evelyn Havir (CAES) for assistance with chlorophyll determinations and pigment analysis via HPLC, and Regan Huntley (CAES) for technical assistance. In addition we thank Maria Moreno (Yale University, New Haven, CT) for assistance with initial cDNA library screening, Donald Miles (University of Missouri, Columbia, MO) for supplying *hcf120* maize lines, and Stephen Dellaporta (Yale) for the *hcf60* maize lines. This work was supported by USDA grant no. 9603819 to Neil Schultes, a BBSRC Research Grant for Ruairidh Sawers to Jane Langdale (University of Oxford, UK), a BBSRC David Phillips Fellowship to Thomas Brutnell (Oxford) and for Roger Krueger an NIH grant no. IR01-6M38148 to Stephen Dellaporta (Yale).

References

Altschul, S.F., Madden, T.L., Schaffer, A.A., Zhang, J., Miller, W. and Lipman, D.L. (1997) Gapped BLAST and PSI-BLAST: a new generation of protein database search programs. *Nucl. Acids Res.* **25**, 3389–3402.

Arnon, D.I. (1949) Copper enzymes in isolated chloroplasts. Polyphenoloxidase in *Beta vulgaris*. *Plant Physiol.* **24**, 1–15.

Ausubel, F.M., Brent, R., Kingston, R.E., Moore, D.D., Siedman, J.G., Smith, J.A. and Struhl, K. (1989) *Short Protocols in Molecular Biology*. New York: John Wiley and Son.

Barkan, A. (1993) Nuclear mutants of maize with defects in chloroplast polysome assembly have altered chloroplast RNA metabolism. *Plant Cell*, **5**, 389–402.

Barkan, A., Walker, M., Nolasco, M. and Johnson, D. (1994) A nuclear mutation in maize blocks the processing and translation of several chloroplast mRNAs and provides evidence for the differential translation of alternative mRNA forms. *EMBO J.* **13**, 3170–3181.

Beckett, J.B. (1978) B–A translocations in maize. *J. Hered.* **69**, 27–36.

Börner, T., Schumann, B. and Hagemann, R. (1976) Biochemical studies on a plastid ribosome-deficient mutant of *Hordeum vulgare*. In *Genetics and Biogenesis of Chloroplasts and Mitochondria* (Bücher, T., Neupert, W., Sebald, W. and Werner, S., eds). Amsterdam: Elsevier, pp. 41–48.

Brutnell, T.P. and Dellaporta, S.L. (1994) Somatic inactivation and reactivation of *Ac* associated with changes in cytosine methylation and transposase expression. *Genetics*, **138**, 213–225.

Brutnell, T.P., Sawers, R.J.H., Mant, A. and Langdale, J.A. (1999) BUNDLE SHEATH DEFECTIVE 2, a novel protein required for post-translational regulation of the *rbcL* gene of maize. *Plant Cell*, **11**, 849–864.

Chen, J. and Dellaporta, S.L. (1993) Urea-based plant DNA miniprep. In *The Maize Handbook* (Freeling, M. and Walbot, V., eds). New York: Springer-Verlag, pp. 526–527.

Christensen, A.H., Sharrock, R.A. and Quail, P.H. (1992) Maize polyubiquitin genes: structure, thermal perturbation of expression and transcript splicing and promoter activity following transfer to protoplasts by electroporation. *Plant. Mol. Biol.* **18**, 675–689.

Cline, K. and Henry, R. (1996) Import and routing of nucleus-encoded chloroplast proteins. *Ann. Rev. Cell Dev. Biol.* **12**, 1–26.

Dabbs, E.R. (1991) Mutants lacking individual ribosomal proteins as a tool to investigate ribosomal properties. *Biochimie*, **73**, 639–645.

Dabbs, E.R., Hasenbank, R., Kastner, B., Rak, K.H., Wartusch, B. and Stöffler, G. (1983) Immunological studies of *Escherichia coli* mutants lacking one or two ribosomal proteins. *Mol. Gen. Genet.* **192**, 301–308.

Dellaporta, S.L. and Moreno, M.A. (1993) Gene tagging with *Ac/Ds* elements in maize. In *The Maize Handbook* (Freeling, M. and Walbot, V., eds). New York: Springer-Verlag, pp. 219–233.

Demmig-Adams, B. and Adams, W.W. (1996) The role of xanthophyll cycle carotenoids in the protection of photosynthesis. *Trends Plant Sci.* **1**, 21–26.

Emanuelsson, O., Nielsen, H. and von Heijne, G. (1999) ChloroP, a neural network-based method for predicting chloroplast transit peptides and their cleavage sites. *Protein Sci.* **8**, 978–984.

Feinberg, A.P. and Vogelstein, B. (1984) A technique for radiolabeling DNA restriction endonuclease fragments to high specific activity. *Anal. Biochem.* **137**, 266–267.

Galili, S., Fromm, H., Aviv, D., Edelman, M. and Galun, E. (1989) Ribosomal protein S12 as a site for streptomycin resistance in *Nicotiana* chloroplasts. *Mol. Gen. Genet.* **218**, 289–292.

Gantt, J.S. and Key, J.L. (1986) Isolation of nuclear plastid ribosomal protein cDNAs. *Mol. Gen. Genet.* **202**, 186–193.

Gantt, J.S. and Thompson, M.D. (1990) Plant cytosolic ribosomal protein S11 and chloroplast ribosomal protein S17. Their primary structures and evolutionary relationships. *J. Biol. Chem.* **265**, 2763–2767.

Golden, B.L., Hoffman, D.W., Ramakrishnan, V. and White, S.W. (1993) Ribosomal protein S17: characterization of the three-dimensional structure by 1H and 15N NMR. *Biochemistry*, **32**, 12812–12820.

Han, C.-D., Coe, E.H., Jr and Martienssen, R. (1992) Molecular cloning and characterization of *iojap* (*ij*), a pattern striping gene of maize. *EMBO J.* **11**, 4037–4046.

Herfurth, E., Hirano, H. and Wittman-Liebold, B. (1991) The amino-acid sequences of the *Bacillus stearothermophilus* ribosomal proteins S17 and S21 and their comparison to homologous proteins of other ribosomes. *Biol. Chem. Hoppe-Seyler*, **372**, 955–961.

Herzog, A., Yaguchi, M., Cabezon, T., Corchuelo, M.C., Petre, J. and Böllen, A. (1979) A missense mutation in the gene coding for ribosomal protein S17 (*rps*Q) leading to ribosomal assembly defectivity in *Escherichia coli*. *Mol. Gen. Genet.* **171**, 15–22.

Hopkins, W.G. and Elfman, B. (1984) Temperature-induced chloroplast ribosome deficiency in virescent maize. *J. Hered.* **75**, 207–211.

Jahn, O., Hartmann, R.K. and Erdmann, V.A. (1991) Analysis of the *spc* ribosomal protein operon of *Thermus aquaticus*. *Eur. J. Biochem.* **197**, 733–740.

Jaishree, T.N., Ramakrishnan, V. and White, S.W. (1996) Solution structure of prokaryotic ribosomal protein S17 by high-resolution NMR spectroscopy. *Biochemistry*, **35**, 2845–2853.

Klaff, P. and Gruissem, W. (1991) Changes in chloroplast mRNA stability during leaf development. *Plant Cell*, **3**, 517–529.

Leon, P., Arroyo, A. and MacKenzie, S. (1998) Nuclear control of plastid and mitochondrial development in higher plants. *Annu. Rev. Plant Physiol. Plant Mol. Biol.* **49**, 453–480.

Mayfield, S.P., Nelson, T. and Taylor, W.C. (1986) The fate of chloroplast proteins during photooxidation in carotenoid-deficient maize leaves. *Plant Physiol.* **82**, 760–764.

McElwain, K.B., Boynton, J.E. and Gillham, N.W. (1993) A nuclear mutation conferring thiostrepton resistance in *Chlamydomonas reinhardtii* affects a chloroplast ribosomal protein related to *Escherichia coli* ribosomal protein L11. *Mol. Gen. Genet.* **241**, 564–572.

Meurer, J., Meierhoff, K. and Westhoff, P. (1996) Isolation of high-chlorophyll-fluorescence mutants of *Arabidopsis thaliana* and their characterization by spectroscopy, immunoblotting and Northern hybridization. *Planta*, **198**, 385–396.

Miles, D. (1994) The role of high chlorophyll fluorescence photosynthesis mutants in the analysis of chloroplast thylakoid membrane assembly and function. *Maydica*, **39**, 35–45.

Mullet, J. (1988) Chloroplast development and gene expression. *Annu. Rev. Plant Physiol. Plant Mol. Biol.* **39**, 475–502.

Peterson, R.B. (1994) Regulation of electron transport in photosystem I and II in C_3, C_3–C_4, and C_4 species of *Panicum* in response to changing irradiance and O_2 levels. *Plant Physiol.* **105**, 349–356.

Peterson, R.B. and Havir, E.A. (2000) A nonphotochemical quenching-deficient mutant of *Arabidopsis* possessing normal pigment composition and xanthophyll cycle activity. *Planta*, **210**, 205–214.

Reiss, T., Bergfeld, R., Link, G., Thien, W. and Mohr, H. (1983) Photooxidative destruction of chloroplasts and its consequences of cytosolic enzyme levels and plant development. *Planta*, **159**, 518–528.

Schultes, N.P., Brutnell, T.P., Allen, A., Dellaporta, S.L., Nelson, T. and Chen, J. (1996) *Leaf permease1* gene of maize is required for chloroplast development. *Plant Cell*, **8**, 463–475.

Somerville, C.R. (1986) Analysis of photosynthesis with mutants of higher plants and algae. *Ann. Rev. Plant Physiol.* **37**, 467–507.

Stern, S., Weiser, B. and Noller, H.R. (1988) Model for the three-dimensional folding of 16S ribosomal RNA. *J. Mol. Biol.* **204**, 447–481.

Stöffler-Meilicke, M., Dabbs, E.R., Albrecht-Erlich, R. and Stöffler, G. (1985) A mutant from *Escherichia coli* which lacks ribosomal proteins S17 and L29 used to localize these two proteins on the ribosome surface. *Eur. J. Biochem.* **150**, 485–490.

Subramanian, A.R. (1993) Molecular genetics of chloroplast ribosomal proteins. *Trends Biochem. Sci.* **18**, 177–181.

Subramanian, A.R., Smooker, P.M. and Giese, K. (1990) Chloroplast ribosomal proteins and their genes. In *The Ribosome. Structure, Function and Evolution* (Hill, W.E., Dahlberg, A., Garrett, R.A., Moore, P.B., Schlessinger, D. and Warner, J.R., eds). Washington: American Society for Microbiology, pp. 655–663.

Sugiura, M., Hirose, T. and Sugita, M. (1998) Evolution and mechanism of translation in chloroplasts. *Ann. Rev. Genet.* **32**, 437–459.

Svab, Z. and Maliga, P. (1991) Mutation proximal to the tRNA binding region of the *Nicotiana* plastid 16S rRNA confers resistance to spectinomycin. *Mol. Gen. Genet.* **228**, 316–319.

Thompson, J.D., Higgins, D.G. and Gibson, T.J. (1994) CLUSTAL W: improving the sensitivity of progressive multiple sequence alignment through sequence weighting, position-specific gap penalties and weight matrix choice. *Nucl. Acids Res.* **22**, 4673–4680.

Thompson, M.D., Jacks, C.M., Lenvik, T.R. and Gantt, J.R. (1992) Characterization of *rps17*, *rps9* and *rps15*: three nucleus-encoded plastid ribosomal protein genes. *Plant Mol. Biol.* **18**, 931–944.

Tokuhisa, J.G., Vijayan, P., Feldmann, K.A. and Browse, J.A. (1998) Chloroplast development at low temperatures requires a homolog of *DIM*1, a yeast gene encoding the 18S rRNA dimethylase. *Plant Cell*, **10**, 699–711.

Urlaub, H., Thiede, B., Müller, E.-C., Brimacombe, R. and Wittmann-Liebold, B. (1997) Identification and sequence analysis of contact sites between ribosomal proteins and rRNA in *Escherichia coli* 30S subunits by a new approach using matrix-assisted laser desorbtion/ionization–mass spectrometry combined with N-terminal microsequencing. *J. Biol. Chem.* **272**, 14547–14555.

Walbot, V. and Coe, E.H., Jr (1979) Nuclear gene *iojap* conditions a programmed change to ribosome-less plastids in *Zea mays*. *Proc. Natl Acad. Sci. USA*, **76**, 2760–2764.

Yaguchi, M. and Wittmann, H.G. (1978) The primary structure of protein S17 from the small ribosomal subunit of *Escherichia coli*. *FEBS Lett.* **87**, 37–40.

Yaguchi, M., Wittmann, H.G., Cabezon, T., De Wilde, M., Villarroel, R., Herzog, A. and Böllen, A. (1976) Alteration of ribosomal protein S17 by mutation linked to neamine resistance in *Escherichia coli*. II. Localization of the amino acid replacement in protein S17 from a *neaA* mutant. *J. Mol. Biol.* **104**, 617–620.

Zubko, M.K. and Day, A. (1998) Stable albinism induced without mutagenesis: a model for ribosome-free plastid inheritance. *Plant J.* **15**, 265–271.